# OPTIMAL CONTROL OF A 3-DOF FREE FLOATING PLATFORM ON A FLAT FLOOR

Carlos M. N. Velosa

*PTP for the European Space Agency (ESA/ESTEC), 2201 AZ Noordwijk, The Netherlands, E-mail: carlos.velosa@esa.int*

## ABSTRACT

This paper presents a control approach based on the optimal control LQR/LQG to control the position and orientation of an air bearing platform with three degrees of freedom (two translational and one rotational) on a flat floor. The approach consists in estimating the state variables of the system resorting to a Kalman estimator and a few measurements and use them in the feedback of the control loop of a LQR with a prescribed degree of stability. Numerical simulations are performed to validate the effectiveness of the controller. The position and orientation of the free floating platform was controlled successfully and the error in the final state (final position and orientation) is negligible taking into account the type of application. This work contributes with the validation of a modern control technique applied to a platform that simulate the motion of satellites before its implementation in real satellites.

**Keywords:** Flat Floor, Air Bearings, Microgravity, Kalman Estimator, LQR, LQG, SATSIM.

## 1 INTRODUCTION

Different methods have been developed over the years to emulate microgravity on the ground. Some are more suitable than others to simulate the dynamics of space platforms as if they were in space. The most accurate microgravity reproduction is the free fall in a vacuum drop tower as can be found for example in ZARM (Center of Applied Space Technology and Microgravity) in Bremen, Germany. However, a main disadvantage of the drop towers is that the microgravity is only available for short periods of time such as 4.74 s as in the case of ZARM [1]. Parabolic flights are another way to achieve microgravity where the tests in microgravity conditions can be carried out for periods of about 20 s [1]. Submerging astronauts or platforms in water is also a common technique. Using this technique the duration of the tests in microgravity can be significantly increased, however one cannot forget that the experiments suffer high drag forces which makes the control of the platforms more difficult. A fourth way to achieve microgravity is resorting to air bearings, a technique that actually has been used since the beginning of the spaceflight [2]. Compressed air is used to create a thin air layer with a few tens of microns between two surfaces minimizing the friction between the bodies.

The Orbital Robotics and GNC (Guidance, Navigation and Control) Laboratory (ORGL) of the European Space Agency in the Netherlands (ESA/ESTEC) is prepared to carry out experiments using air bearing platforms. The laboratory is equipped with an extremely flat floor, made of epoxy, with an area of 45 $m^2$ (9m x 5m), where the maximum height difference between two extreme points of the flat floor is about 0.8 mm, a floor which due to its characteristics, mainly size and flatness, is unique in Europe. Such a facility, together with platforms featuring planar air bearings, allow the platforms to move with three degrees of freedom: two translational and one rotational (motion in the plane).

The flat floor is in the field of view 14 VICON cameras, a motion tracking system that resorting to small reflective markers placed in a given object allows the absolute motion tracking in real-time of that object with submillimetre precision. A minimum set of four markers are needed to track the pose and this system can be used to provide the position and the orientation of the platform for control purposes.

A platform with four air bearings and eight thrusters is available in the laboratory to be used as a control testbed. Designated by SATSIM (Satellite Control Simulator Platform), the platform has a mass of $m = 198.5$ kg (with a pressure in the tanks of 250 bar), a moment of inertia around the axis of symmetry (the vertical axis, $z$, perpendicular to the ground) of $I_{zz} = 11.5\ \text{kg.m}^2$, and has a payload capacity that goes up to 50 kg. The four air bearings that lift the platform are connected to a hose that provides pressurized air from an external pneumatic system, being this pressure locally regulated to between 6 and 6.8 bar depending on the load of the platform. The thrusters are aligned with the four cardinal directions of the platform, providing thrust in the $x$ and $y$ directions, and they work with a pressure of 8 bar. Fig.1 shows the platform on the flat floor:

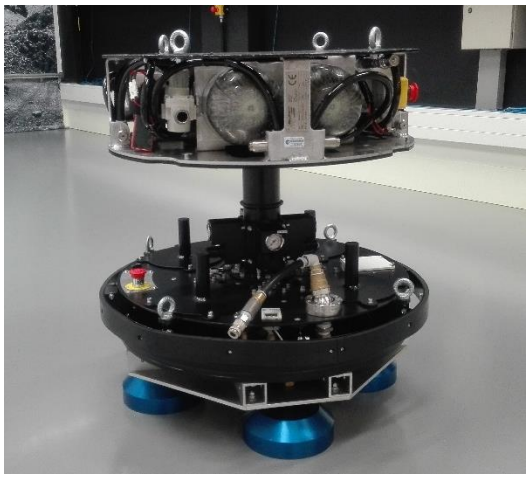

*Figure 1: SATSIM air bearing platform in the ORGL flat floor.*

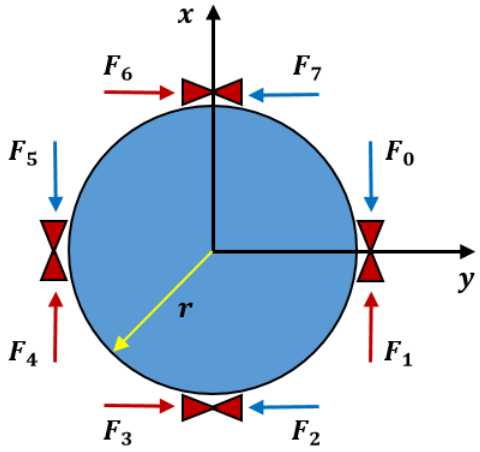


*Figure 2: Disposition of the thrusters on the platform.*

The purpose of the present paper is to present a control approach to control the position and the orientation of a free floating platform on a flat floor, simulating therefore the motion control of a satellite restricted to a bi-dimensional space. The work is motivated by the fact that satellite servicing has become one of the today's space challenges. The need to develop technologies to approach, grasp, manipulate, modify, repair, refuel, integrate and build new platforms and spacecraft on orbit became one of the priorities of the space agencies. By way of example nowadays satellites cannot be refuelled in orbit, meaning that they must carry all the fuel they need for the entire lifetime. In this context, ESA is currently working on a project to change that, by developing a mechanism which will allow to grab a satellite in orbit and pass fuel to it through a tanker spacecraft. So, control approaches must be tested before their implementation in real satellites.

The paper is organized as follows: the problem to be solved is stated in section 2, which is the control of the position and orientation of a free floating platform; in section 3, a solution to the problem is presented, which is the control of the platform based on the optimal control LQR/LQG (Linear-Quadratic Regulator / Linear-Quadratic-Gaussian) with a prescribed degree of stability; the section 4 deals with the validation of the control through numerical simulations; and the paper ends, lastly, in section 5 with the main conclusions about the results.

## 2 PROBLEM STATEMENT

### 2.1 Dynamical Model

Let Fig.2 represent the disposition of the thrusters on the platform SATSIM. The force exerted by each thruster is represented close to the respective thruster. By convention the $x$-axis points forward, the $y$-axis points to the right and the $z$-axis points down. The radius of the platform is denoted by $r$.

Considering that there are no external disturbances, which is a reasonable simplification if one considers that there is no friction between the platform and the floor, the dynamical model of the platform can be obtained resorting to the second law of Newton:

$$\ddot{x} = F_x/m \qquad \ddot{y} = F_y/m \qquad \ddot{\theta} = T_z/I_{zz} \tag{1}$$

where $\ddot{x}$ and $\ddot{y}$ denote the accelerations in the $x$ and $y$ directions, $F_x$ and $F_y$ the total forces in the $x$ and $y$ directions, $m$ the mass of the platform, $I_{zz}$ the moment of inertia around the $z$-axis, and $T_z$ the torque applied to the platform around the $z$-axis.

By performing the change of variables $\dot{x} = u$, $\dot{y} = v$ and $\dot{\theta} = \omega$, the dynamics of the system can be written in the form of ordinary differential equations:

$$\begin{aligned} \dot{x} &= u \\ \dot{y} &= v \\ \dot{u} &= F_x/m \\ \dot{v} &= F_y/m \\ \dot{\theta} &= \omega \\ \dot{\omega} &= T_z/I_{zz} \end{aligned} \tag{2}$$

with:

$$F_x = F_1 + F_4 - F_0 - F_5 \tag{3}$$

$$F_y = F_3 + F_6 - F_2 - F_7 \tag{4}$$

$$T_z = (F_0 + F_2 + F_4 + F_6 - F_1 - F_3 - F_5 - F_7) \times r \tag{5}$$

wherein $x$ and $y$ represent the position of the platform on the flat floor, $u$ and $v$ the velocities along the $x$ and $y$ directions, respectively, $\theta$ the orientation of the platform, and $\omega$ the angular velocity.

### 2.2 PWM Signals to the Thrusters

The platform rely on ON-OFF thrusters to control its position and orientation and the outputs of any controller are continuous signals in time. There is therefore the need to transform the continuous forces provided by the controller in ON-OFF forces, which can be achieved resorting to a PWM (Pulse Width Modulation). In a PWM signal, the average value of the force exerted by a thruster is controlled by turning on and off the solenoid valves at a fast rate and the longer the thruster is ON compared to the OFF periods, the higher is the total force provided by the thruster. Fig.3 shows a PWM signal indicating if the thruster is ON or OFF.

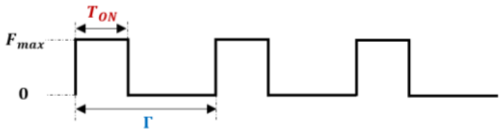


*Figure 3: Force exerted by a thruster in the form of a PWM signal: thruster ON, thruster OFF.*

The Duty Cycle ($DC$) of a PWM signal is expressed as the ratio between the pulse width, $T_{ON}$, that is, the time for which the signal is ON, and the total period of the signal, Γ:

$$DC = \frac{T_{ON}}{\Gamma} \times 100\% \quad (6)$$

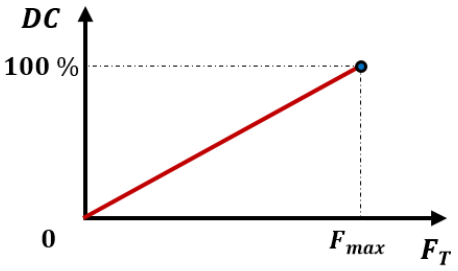


*Figure 4: Representation of the Duty Cycle, $DC$, as a function of the force exerted by the thruster, $F_T$.*

Since the purpose is to have a duty cycle of $DC = 100\%$ for the maximum force, $F_{max}$, that is, the thruster completely open for the entire period, Γ, of the PWM signal, the slope 'm' of the line relating the duty cycle, $DC$, with the force exerted by the thruster, $F_T$, see Fig.4, is given as $m = \Delta y/\Delta x = (100\% - 0\%)/(F_{max} - 0)$, and with this the duty cycle can be written as a function of the force as $DC = 100\%/F_{max} \times F_T$. Substituting this expression in Eq.6 and resolving in order to the pulse width, $T_{ON}$, yields in the following expression which relates the pulse width with the force exerted by the thruster:

$$T_{ON} = \frac{F_T}{F_{max}} \times \Gamma \quad (7)$$

## 3 APPROACH PROPOSED

Denoting the state vector $x = [x_1, \dots, x_6]^T = [x, y, u, v, \theta, \omega]^T$ and the control vector $u = [u_1, \dots, u_8]^T = [F_0, \dots, F_7]^T$ the system (2), $\dot{x} = f(x, u)$, can be written in the form of a linear time-invariant system, $\dot{x} = Ax + Bu$, with matrices $A$ and $B$ given by the Jacobians:

$$A = \frac{\partial f}{\partial x} = \begin{bmatrix} \frac{\partial f_1}{\partial x_1} & \cdots & \frac{\partial f_1}{\partial x_6} \\ \vdots & \ddots & \vdots \\ \frac{\partial f_6}{\partial x_1} & \cdots & \frac{\partial f_6}{\partial x_6} \end{bmatrix}_{x=x_{eq}\,;\,u=u_{eq}}$$

$$B = \frac{\partial f}{\partial u} = \begin{bmatrix} \frac{\partial f_1}{\partial u_1} & \cdots & \frac{\partial f_1}{\partial u_8} \\ \vdots & \ddots & \vdots \\ \frac{\partial f_6}{\partial u_1} & \cdots & \frac{\partial f_6}{\partial u_8} \end{bmatrix}_{x=x_{eq}\,;\,u=u_{eq}} \quad (8)$$

where $x_{eq}$ and $u_{eq}$ denote the state vector and the control vector, respectively, in the equilibrium, $\dot{x} = Ax_{eq} + Bu_{eq} = 0$.

### 3.1 LQR with a Specified Degree of Stability

For a controllable, linear, time-invariant system given as follows:

$$\begin{aligned} \dot{x} &= Ax + Bu \\ y &= Cx \end{aligned} \quad (9)$$

with initial condition $x(t_0) = x_0$ and no final time constraint, it is well-known from the optimal control theory that the control law which steers the trajectory to the equilibrium state, $x_{eq}$, minimizing the performance index:

$$J = \frac{1}{2}\int_{t_0}^{\infty} e^{2\gamma t}\,(x^T Q x + u^T R u)dt \;,\; \gamma \geq 0 \quad (10)$$

is given by Eq.11, [3], [4]:

$$u = u_{eq} - K(x - x_{eq}) \quad (11)$$

where the gain matrix of the controller, $K$, is computed as $K = R^{-1}B^T P$, with $P \in \mathbb{R}^{n\times n}$ being a symmetric and positive definite matrix ($P = P^T, P > 0$), solution of the Algebraic Riccati Equation (ARE):

$$P(A + \gamma I) + (A + \gamma I)^T P - PBR^{-1}B^T P + Q = 0 \quad (12)$$

wherein $Q \in \mathbb{R}^{n\times n}$ and $R \in \mathbb{R}^{m\times m}$ are two weighting matrices, being $Q$ symmetric and positive semi-definite ($Q = Q^T, Q \geq 0$) and $R$ symmetric and positive definite ($R = R^T, R > 0$), and $\gamma \geq 0$ a scalar number denoting the specified degree of

stability. The robustness of the LQR is assured by the parameter $\gamma$ given that $\gamma$ causes a $\gamma$-shift in the eigenvalues of the closed-loop matrix $\bar{A} = A - BR^{-1}B^T P$ to the left in the direction of the real axis.

### 3.2 Determination of the Weighting Matrices Q and R

The determination of the weighting matrices $Q$ and $R$ aims to find the respective matrices that minimize the cost function (10). According to the Bryson's rule, the matrices $Q$ and $R$ are composed only by their main diagonals and each element is equal to the inverse of the maximum value of each squared variable [5], [6]. Thus, for a state vector of dimension $n$, $x = [x_1, \dots, x_n]^T$, and for a control vector of dimension $m$, $u = [u_1, \dots, u_m]^T$, the matrices $Q: [n \times n]$ and $R: [m \times m]$ that minimize the cost function $J$ take the following form:

$$Q = \begin{bmatrix} 1/x_{1,max}^2 & 0 & 0 & 0 \\ 0 & 1/x_{2,max}^2 & 0 & 0 \\ 0 & 0 & \ddots & 0 \\ 0 & 0 & 0 & 1/x_{n,max}^2 \end{bmatrix} \quad (13)$$

$$R = \begin{bmatrix} 1/u_{1,max}^2 & 0 & 0 & 0 \\ 0 & 1/u_{2,max}^2 & 0 & 0 \\ 0 & 0 & \ddots & 0 \\ 0 & 0 & 0 & 1/u_{m,max}^2 \end{bmatrix}$$

### 3.3 Observer / Kalman Estimator

Consider a system given by the following mathematical model:

$$\begin{aligned} \dot{x} &= Ax + Bu + Fw \\ y &= Cx + v \end{aligned} \quad (14)$$

where $x \in \mathbb{R}^n$ denotes the state vector, $u \in \mathbb{R}^m$ the control vector, $y \in \mathbb{R}^p$ the output vector (the measured outputs available for feedback), $A \in \mathbb{R}^{n \times n}$ the state matrix, $B \in \mathbb{R}^{n \times m}$ the control matrix, $C \in \mathbb{R}^{p \times n}$ the output matrix, and $F \in \mathbb{R}^{n \times n}$ an input matrix. $w \in \mathbb{R}^n$ and $v \in \mathbb{R}^p$ represent respectively the process and measurement noise that affect the system and they are assumed to be independent White Gaussian Noises (WGN), that is, uncorrelated noises, $E\{w_i w_j^T\} = E\{v_i v_j^T\} = 0$, $i \neq j$, with zero mean, $E\{w\} = E\{v\} = 0$, and with a Gaussian distribution.

Let the stochastic variables $w$ and $v$ be characterized by the respective covariance matrices (noise levels) $Q_k \in \mathbb{R}^{n \times n}$ and $R_k \in \mathbb{R}^{p \times p}$, being described as diagonal matrices composed by the variances of each variable:

$$E\{ww^T\} = Q_k = \begin{bmatrix} \sigma_1^2 & 0 & 0 \\ 0 & \ddots & 0 \\ 0 & 0 & \sigma_n^2 \end{bmatrix}$$

$$E\{vv^T\} = R_k = \begin{bmatrix} \sigma_1^2 & 0 & 0 \\ 0 & \ddots & 0 \\ 0 & 0 & \sigma_p^2 \end{bmatrix} \quad (15)$$

In complex systems, the covariance matrix of the noise of the process, $Q_k$, and the covariance matrix of the noise of the sensors, $R_k$, change over time depending on the disturbances that affect the system and the sensors. However, $Q_k$ and $R_k$ are considered constant over time in this paper to simplify the formulation of the filter.

For the perturbed system (14), the equation of an optimal observer/estimator that estimates all the sate variables of the system, $\hat{x}$, with the property that $\hat{x}(t) \to x(t)$ as $t \to \infty$, resorting to the control inputs, $u$, and to the outputs of the system corrupted with noise, $y$, is given by [7]:

$$\dot{\hat{x}} = A\hat{x} + Bu + L(y - C\hat{x}) \quad (16)$$

where $L$ is the gain matrix of the estimator and should be determined in such a way that the matrix $A - LC$ has eigenvalues with negative real parts.

Notice the similarity between designing a state feedback controller and designing an estimator. In a state feedback controller by eigenvalue assignment, the objective boils down to find a matrix $K$ such that the matrix $A - BK$ has eigenvalues with negative real parts, and in an estimator the objective boils down to find a matrix $L$ such that the matrix $A - LC$ has also eigenvalues with negative real parts.

In fact, an estimator can be formulated resorting to a dual space of a system. A dual space is a virtual space, which does not represent the system physically, but that allows to find the matrix $L$ of the estimator in an easy way. The relationship between the primal space and the dual space is that a controllable system in the primal space corresponds to an observable system in the dual space, and that a controllable system in the dual space corresponds to an observable system in the primal space. This way, one can resort to the dual space to find the matrix $L$. By implementing a controller in the dual space, we are automatically implementing an estimator in the primal space.

Thus, the matrix $L$ can be obtained in several ways, depending on the type of controller chosen in the dual space. If $L$ is obtained by the LQR controller, the estimator is called Kalman estimator, and if $L$ is obtained by other controller or by other tecnhique (e.g.: pole placement), the estimator is simply called estimator.

Being the estimator design problem the dual of the state feedback design problem, one has the following equivalence between matrices [7]:

$$A \leftrightarrow A^T \quad , \quad B = C^T \quad , \quad K = L^T \qquad (17)$$

In the dual space, the equation of the error of the state becomes:

$$\dot{e}_x^d = A^T e_x^d + C^T v \qquad (18)$$

where $v$ denotes the control vector of the error. The dual error, $e_x^d$, is forced to stabilize in zero by finding the gain matrix of a closed loop controller, $L^T$, with the control law $v = -L^T e_x^d$. In the theory of the LQR controllers the matrix $L^T$ is calculated as:

$$L^T = R_k^{-1} C P \qquad (19)$$

whose matrix $P \in \mathbb{R}^{n \times n}$ is a symmetric and positive definite matrix ($P = P^T, P > 0$), solution of the Algebraic Riccati Equation (ARE):

$$AP + PA^T - PC^T R_k^{-1} CP + Q_k = 0 \qquad (20)$$

With all the state variables of the system estimated by Eq.16, $\hat{x}$, the state vector, $x$, in the control law (11) is substituted by the estimated state vector, $\hat{x}$, becoming:

$$u = u_{eq} - K(\hat{x} - x_{eq}) \qquad (21)$$

The procedure by which a Linear-Quadratic Regulator (LQR) and a linear quadratic estimator (Kalman estimator) are designed separately for a linear time-invariant system and then put together to form a feedback control loop is referred to as the Linear-Quadratic-Gaussian controller (LQG).

## 4 SIMULATION RESULTS

For simulation purposes the ordinary differential equations (2) and (16) are solved simultaneously through the Runge-Kutta-Butcher method [8] between $t_0 = 0$ and $t_f = 120$ s (2 min), with a step of $\Delta t = 10$ ms, and departing from the initial conditions (22). The control is turned on in the beginning of the simulation, at $t_{u_{on}} = 0$ s, to steer the platform from the initial state, $x_0$, to the specified equilibrium state, $x_{eq}$.

The output signals of the controller, $u = [F_0, \dots, F_7]^T$, are, in a first stage, continuous signals because they are a result of the feedback law (21). Given the nature of the control law, these control signals can be positive or negative, but the real signals/forces that can be applied to the platform must be positive because the thrusters do not change their directions (fixed directions). On the other hand, the real forces must be in the form of a PWM because the thrusters cannot provide continuous forces in time. The thrusters are ON or OFF, providing zero or the maximum thrust available. Considering this, a saturation function together with the PWM function (7) were implemented after the controller.

Moreover, the thrusters have a given response capability due to the opening and closing times of the solenoid valves. According to the respective datasheet, a minimum pulse width of $T_{ON,min} = 20$ ms was taken into consideration. The period of the PWM signals was chosen as $\Gamma_{PWM} = 200$ ms.

The working pressure of the thrusters is $P_{reg} = 8$ bar (800 kPa) and the exit diameter of the nozzles is $d = 3.9$ mm , $A_e = \pi.(d/2)^2 = 1.195 \times 10^{-5}$ m$^2$. The theoretical force produced by each thruster results in $F_{max} = 13.58$ N. In order to design the controller, the maximum force, $F_{max}$, is needed. For simulation purposes it was considered $F_{max} = 10$ N.

The thrusters are located at a radius of $r = 32.8$ cm from the centre of rotation of the platform, expression (5).

Initial conditions:

$$\begin{gathered} x_0 = [x \ y \ u \ v \ \theta \ \omega]^T = \\ = [-1 \ -1 \ 0 \ 0 \ 45.\pi/180 \ 0.\pi/180]^T \\ \hat{x}_0 = \left[\hat{x} \ \hat{y} \ \hat{u} \ \hat{v} \ \hat{\theta} \ \hat{\omega}\right]^T = \\ = [0 \ 0 \ 0 \ 0 \ 0.\pi/180 \ 0.\pi/180]^T \end{gathered} \qquad (22)$$

Equilibrium state:

$$\begin{gathered} x_{eq} = [x \ y \ u \ v \ \theta \ \omega]^T = \\ = [0 \ 0 \ 0 \ 0 \ 0.\pi/180 \ 0.\pi/180]^T \end{gathered} \qquad (23)$$

Controller parameters:

$$\gamma = 0.6$$

$$\begin{gathered} Q = \text{diag}\left(\left[\frac{1}{x_{max}^2} \ \frac{1}{y_{max}^2} \ \frac{1}{u_{max}^2} \right.\right. \\ \left.\left. \frac{1}{v_{max}^2} \ \frac{1}{\theta_{max}^2} \ \frac{1}{\omega_{max}^2}\right]\right) \\ R = \text{diag}\left(\left[\frac{1}{F_{0,max}^2} \ \frac{1}{F_{1,max}^2} \ \dots \ \frac{1}{F_{7,max}^2}\right]\right) \end{gathered} \qquad (24)$$

with: $x_{max} = y_{max} = 5.0$ m , $u_{max} = v_{max} = 0.10$ m/s, $\theta_{max} = 360.\pi/180$ rad, $\omega_{max} = 10.\pi/180$ rad/s, and $F_{0,max} = F_{1,max} = \dots = F_{7,max} = 10$ N. The gain matrix of the LQR controller, $K$, was obtained resorting to the Matlab function available in the control system toolbox: $K = lqr(A + \gamma.I_{6\times6}, B, Q, R)$.

Kalman Estimator Parameters:

$$Q_k = \text{diag}\left(\left[\sigma_x^2 \;\; \sigma_y^2 \;\; \sigma_u^2 \;\; \sigma_v^2 \;\; \sigma_\theta^2 \;\; \sigma_\omega^2\right]\right) = \\ = (10^{-2})^2 . I_{6\times 6}$$
$$R_k = \text{diag}\left(\left[\sigma_x^2 \;\; \sigma_y^2 \;\; \sigma_\theta^2\right]\right) = (10^{-2})^2 . I_{3\times 3} \quad (25)$$

The output matrix, $C$, is chosen such that $y = [x\ y\ \theta]^T$, wherein $y = Cx$, with $x = [x\ y\ u\ v\ \theta\ \omega]^T$. This results:

$$C = \begin{bmatrix} 1 & 0 & 0 & 0 & 0 & 0 \\ 0 & 1 & 0 & 0 & 0 & 0 \\ 0 & 0 & 0 & 0 & 1 & 0 \end{bmatrix} \quad (26)$$

Independent measurement noise with zero mean and standard deviation $\sigma = 10^{-2}$ was considered in the three measured variables $(x, y, \theta)$, that is, noise $v_i$, $i = 1, \ldots, 3$, with $\sigma_x = \sigma_y = \sigma_\theta = 10^{-2}$, and process noise in the dynamics of the system $(\dot{x}, \dot{y}, \dot{u}, \dot{v}, \dot{\theta}, \dot{\omega})$, that is, noise $w_j$, $j = 1, \ldots, 6$, with $\sigma_x = \sigma_y = \sigma_u = \sigma_v = \sigma_\theta = \sigma_\omega = 10^{-2}$ was considered in the simulations.

The results of the numerical simulations are shown in Figs.5-10. Figs.5-8 represent the time evolution of the state variables of the system. Fig.5 represents the position $(x, y)$ of the platform on the flat floor, Fig.7 the linear velocity $(u, v)$ in the $x$ and $y$ directions, respectively, Fig.6 the orientation of the platform, described by the angle of rotation, $\theta$, and Fig.8 the respective angular velocity, $\omega$. In the mathematical equations the govern the motion of the system, the rotation, $\theta$, and the angular velocity, $\omega$, are expressed in rad and rad/s, respectively. However, $\theta$ and $\omega$ are shown in Figs.6 and 8 in degrees and degrees/s for a better physical interpretation of the results. In Figs.5-6, the plots show also the outputs of the system, $y = [x, y, \theta]^T$, that is, the state variables that are measured, $(x, y, \theta)$. The remaining state variables, $(u, v, \omega)$ are estimated through the Kalman estimator. In blue it is represented the measured variables, in black the estimated variables, and in red the calculated variables through the dynamics of the system. Figs.9-10 show the control variables of the system in the form of a PWM, that is, the real forces, $F_0, \ldots, F_7$, exerted by the thrusters to control the platform.

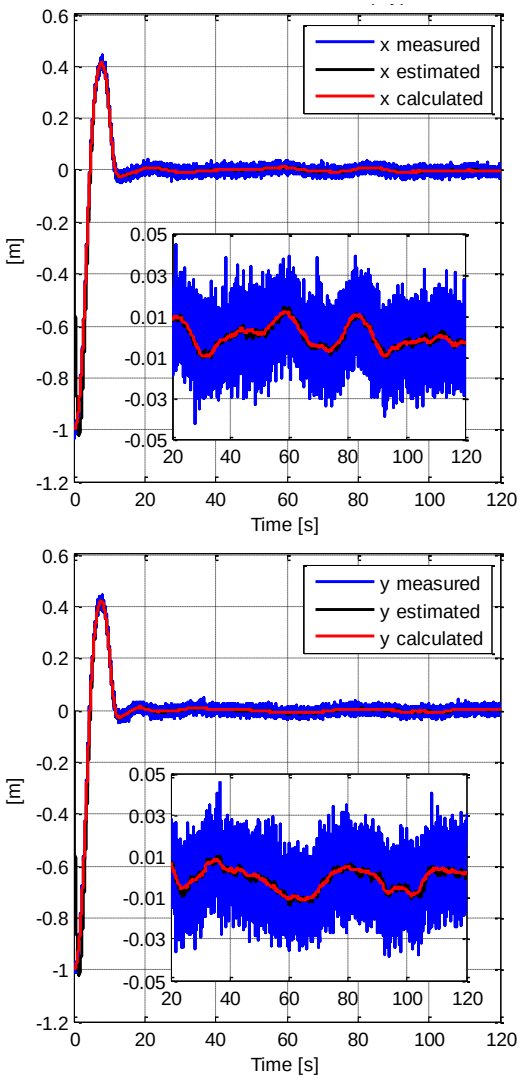


*Figure 5: Position $(x, y)$ of the platform.*

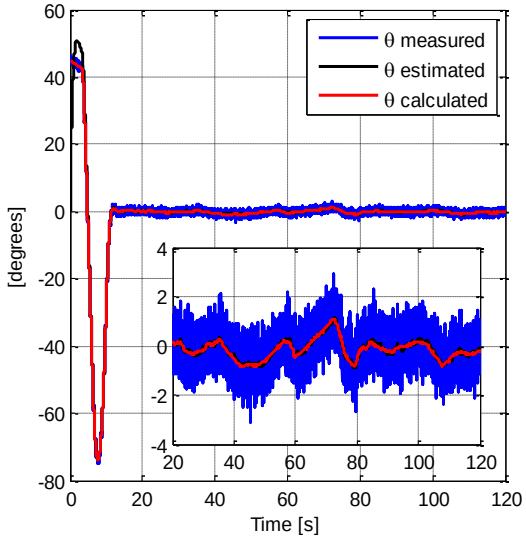


*Figure 6: Orientation / rotation $(\theta)$ of the platform.*

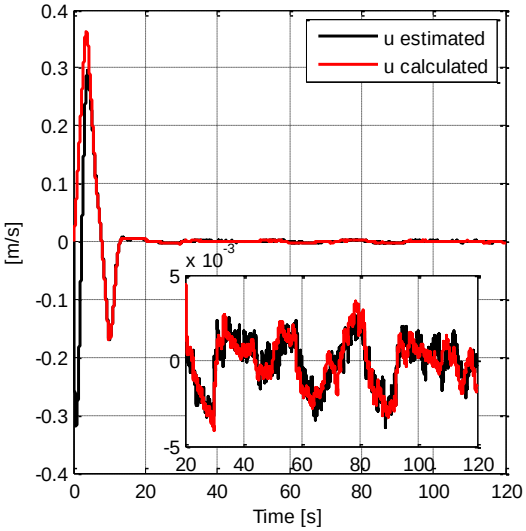


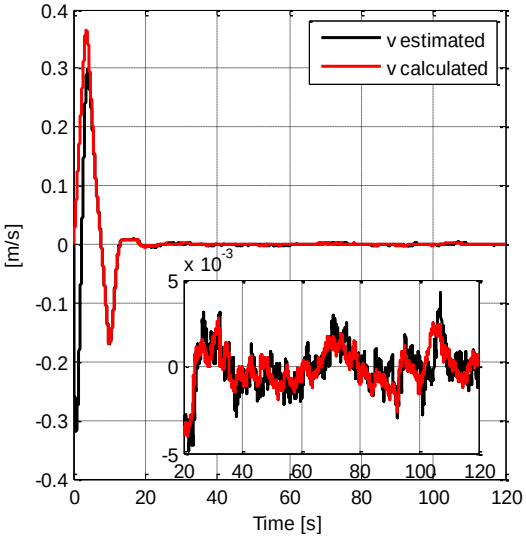


*Figure 7: Linear velocity $(u, v)$ of the platform.*

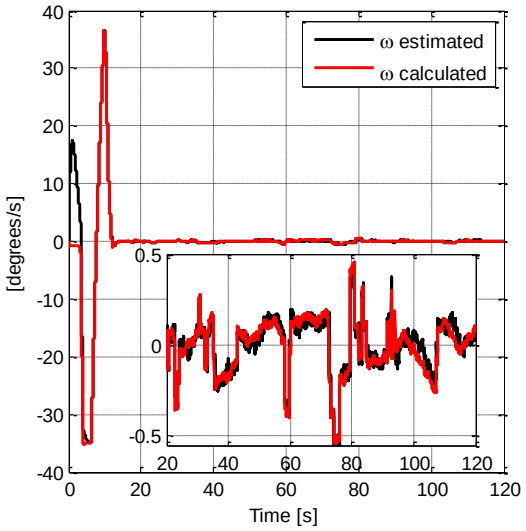


*Figure 8: Angular velocity $(\omega)$ of the platform.*

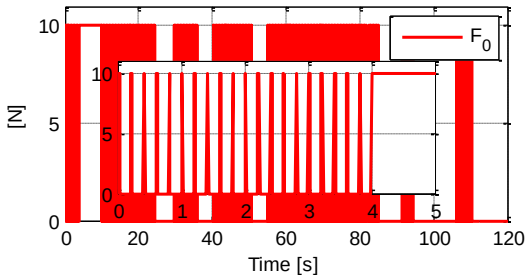


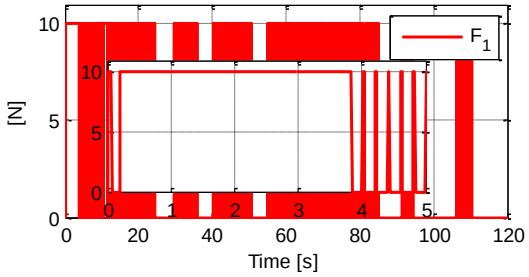


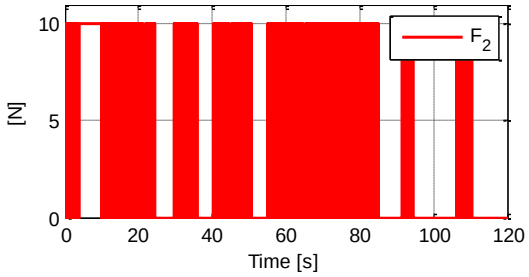


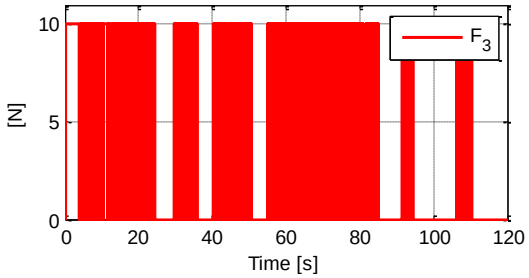


*Figure 9: Forces of the thrusters. Thrusters $F_0$ to $F_3$.*

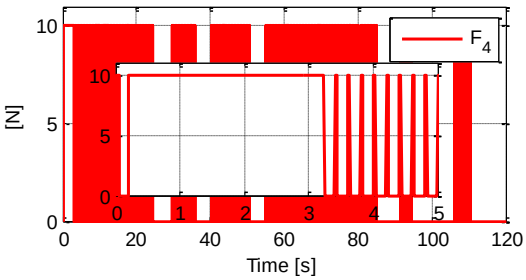

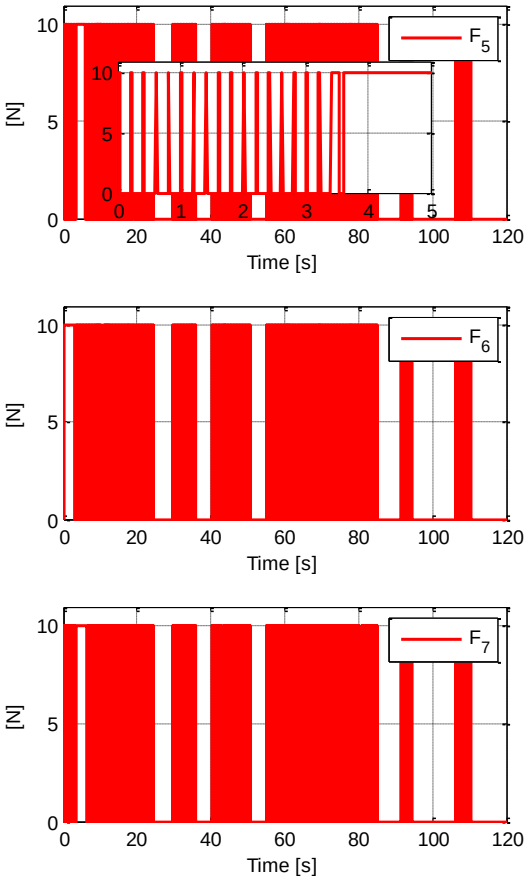


*Figure 10: Forces of the thrusters. Thrusters $F_4$ to $F_7$.*

## 5 CONCLUSIONS

In this paper a LQR/LQG controller to control the position and orientation of a three degree of freedom satellite simulator has been presented. The simulator concerned consists of an air bearing platform that floats freely on a flat floor, simulating therefore the motion of a satellite in two dimensions in a microgravity environment. The control is achieved by combining a Kalman estimator, which estimates all the state variables of the system resorting to the position of the platform, with the modern control technique LQR.

Numerical simulations are carried out to validate the effectiveness of the method and to tune the parameters of the controller. All the parameters of the controller are computed offline. The numerical simulations show that the position and orientation of the platform are successfully controlled, remaining stable in the sense of Lyapunov (only with a small error) in the final state. However, this small error is acceptable taking into account the dimensions of the flat floor (the space where the platform can move) and the objective of the control.

The thrusters are controlled with PWM signals and it occurs that a minimum impulse given by one of the thrusters when the platform is in the final state (final position and orientation) is enough to deviates the platform from the desired final state. This is why there is a small error in the final state.

The present work contributes with the validation of an optimal control approach in a powerful platform that simulates the motion of a satellite in microgravity scenarios in a unique facility of the European Space Agency (ESA).

## Acknowledgments

This research was conducted in the Automation & Robotics Section of the European Space Research and Technology Centre of the European Space Agency (ESA/ESTEC) in Noordwijk, the Netherlands, and supported by the Portuguese Foundation for Science and Technology (FCT) through the following program:

## References

[1] H. Kolvenbach and K. Wormnes, "Recent Developments on ORBIT, a 3-DOF Free Floating Contact Dynamics Testbed," in *13th International Symposium on Artificial Intelligence, Robotics and Automation in Space (i-SAIRAS 2016)*, 2016, pp. 1–7.

[2] J. Schwartz, M. Peck, and C. Hall, "Historical Review of Air-Bearing Spacecraft Simulators," *J. Guid. Control. Dyn.*, vol. 26, no. 4, pp. 513–522, 2003.

[3] D. S. Naidu, *Optimal Control Systems*, 1st ed. CRC Press, 2002.

[4] K. Bousson and C. M. N. Velosa, "Robust Control and Synchronization of Chaotic Systems with Actuator Constraints," in *Handbook of Research on Artificial Intelligence Techniques and Algorithms*, P. Vasant, Ed. IGI Global, 2014, pp. 1–43.

[5] S. K. Choudhary, "LQR Based PID Controller Design for 3-DOF Helicopter System," *Int. J. Comput. Electr. Autom. Control Inf. Eng.*, vol. 8, no. 8, pp. 1498–1503, 2014.

[6] M. Azkarate, "Optimal Formation Flight Control Using Coupled Inter-Spacecraft Dynamics," M.Sc. Thesis, Massachusetts Institute of Technology (M.I.T.), 2009.

[7] K. J. Aström and R. M. Murray, *Feedback Systems: An Introduction for Scientists and Engineers*. New Jersey: Princeton University Press, 2010.

[8] J. Y. Park, D. J. Evans, K. Murugesan, and S. Sekar, "Optimal Control of Time-Varying Singular Systems Using the RK-Butcher Algorithm," *Int. J. Comput. Math.*, vol. 82, no. 5, pp. 617–627, 2005.